The Influence of Environmental Factors on Land Surface Temperature in Taichung City

Ya-Yun Xiao[1], Yi-Shiang Shiu[2], Re-Yang Lee[3]

[1] Master's Program of Landscape &Recreation, Feng Chia University,

No. 100, Wenhwa Rd., Seatwen, Taichung, Taiwan 40724 (R.O.C.)

Email: Hsiao.19921026@gmail.com

[2]Department of Urban Planning and Spatial Information, Feng Chia University

No. 100, Wenhwa Rd., Seatwen, Taichung, 40724 Taiwan (R.O.C.)

Email: ysshiu@fcu.edu.tw

[3]Department of Land Management, Feng-Chia University

No. 100, Wenhwa Rd., Seatwen, Taichung, 40724 Taiwan (R.O.C.)

e-mail: rylee@fcu.edu.tw

KEYWORDS: Land surface temperature retrieval, Spatial autocorrelation, Spatial regression analysis models

ABSTRACT: Studies have proven that several local environmental factors (such as land use, land cover, and solar radiation) can influence the daytime land surface temperature (LST). Therefore, modulating these key factors can help mitigate urban heat island (UHI) effects. However, other factors from neighboring areas rather than the local area influence the local LST. To identify the factors from neighboring areas, we must answer two research questions: (1) Does the LST of an area influence those of its neighboring areas? (2) Is the LST of an area influenced by the environmental factors of neighboring areas? Therefore, the purpose of this study was to explore the relationship between LST and land surface environment by using spatial autoregressive models including the spatial lag model and spatial error model. Taichung City, the third-largest city in Taiwan, was selected as the study area. The predisposing environmental factors that could influence LST were retrieved by investigating data on Landsat series thermal imagery and land use. Factors that were significant during different periods from 2010 to 2015 were selected to predict the cooling effects after increasing green cover in specific areas: Maple Garden, the National Taichung Theater, People's Square, the IKEA green roof, Green Park Road, and other large-scale green-space planning projects. Future applications include optimizing green-space locations to reduce daytime UHI effects.

1. INTRODUCTION

Because of industrial revolution and urbanization, built-up areas have expanded, which has resulted in the reduction of green areas. Impermeable pavement and cement buildings prevent land from quick heat dissipation, which results in the urban heat island (UHI) effect.

Taichung City is the second-largest city in Taiwan because of its role as a traffic hub, and its urban areas are rapidly expanding. In recent years, Taichung City Government has approved many green land planning measures.

Therefore, exploring Taichung City's high-density-area land surface temperature (LST) and UHI effect has become crucial. Accordingly, we used the Landsat series of satellite images to monitor the UHI effect.

According to a review of the literature, many causes of the high-temperature UHI effect have been proposed. Howard proposed the UHI effect in 1833. In urban areas, numerous buildings, impermeable pavement, and a lack of green land lead to the UHI effect. Cement buildings usually absorb substantial solar radiation during the daytime and increase the urban temperature. In the nighttime, the impervious pavement cannot absorb the solar radiation, and thus, the internal temperature cannot be reduced. Recently constructed high-rise buildings feature geometric characteristics, numerous glass curtains, and cement, which increase atmospheric radiation and alter the surface reflection path. Additionally, high-rise buildings cause wind resistance and prevent airflow from completing parallel convection, which allows urban areas to easily retain high temperatures (Chang, 2010).

Numerous studies have confirmed that green land can effectively reduce LST and the UHI effect because green land can absorb solar radiation and increase heat evapotranspiration and offer shade while reducing urban temperatures. This is called the urban cold island effect. Urban green land can effectively improve the city environment by adjusting its microclimate, improving air quality, reducing the UHI effect, reducing the impact of environmental developments, and repairing the ecological chain (Chang, 2010). For example, New York's Central Park is known as the "lungs of New York City."

From the literature, we classified many factors that affect the urban environment (Chang, 2010; Landsberg, 1981; C.-M. Lin, 2010; H.-T. Lin, Kuo, Lee, Chen, &Chen, 2001; Lu, 2008), including excessive energy use, emissions, green land reduction, and suspended particulates, and we assumed that the key factors influencing the UHI in the city are vegetation, water, buildings, average solar radiation, and sky view factor (Bottyn & Unger, 2003; Chun & Guldmann, 2014; Landsberg, 1981).

In this study, we selected Taichung City as the study area; Landsat series images were used as the data sources. We used spatial and nonspatial regression models, including the ordinary least squares (OLS) estimator, spatial error model (SEM), and spatial lag model (SLM) to explore the relationship between LST and the six key factors. Landsat 4-5 TM in December 2010 and Landsat 8 OLI in December 2015 were used to retrieve the LST and normalized difference vegetation index (NDVI)(Anselin, 2013; Song, Du, Feng, & Guo, 2014). Regression models built using the data of 2010 and 2015 were used to predict the future LST after green land planning.

2. DATA PROCESSING AND RESEARCH METHODS

2.1 DATA PROCESSING

2.1.1 Building

We used a topographic map to digitize street maps of buildings and obtain information on buildings (e.g., height, area, and floors). The building ground floor area (BGFA) is the sum of the ground floor areas of all buildings in a given unit area (cell) and equals the total building rooftop area given by (Chun & Guldmann, 2014):

$$\mathrm{BGFA} = \sum_{i=1}^{n} ai \quad ,$$

where ai is building i's ground floor area in a given cell and n is the number of building footprints.

2.1.2 Water

Water can reduce LSTs, and it exists in liquid, solid, gaseous, and other forms. Because water is highly correlated with NDVI, this study separated the NDVI and water factors. An NDVI value approaching −1 can be used to

identify water and to represent impermeable pavement. The NDVI is defined as follows (Xu, 2006):

$$\text{NDVI} = \frac{Green - NIR}{Green + NIR},$$

where *NIR* is a near infrared ray with a wavelength of 0.86 μm.

2.1.3 NDVI

NDVI has been used in many studies on UHI effects because plants and heat radiation have a cool island effect. NDVI ranges from 1 to −1 and usually signifies vegetation cover. An NDVI value close to 1 signifies intensive vegetation coverage, whereas a value closer to 0 signifies bare land. The NDVI is defined as follows (Carlson & Ripley, 1997):

$$\text{NDVI} = \frac{NIR - Red}{NIR + Red},$$

where *NIR* is a near infrared ray with a wavelength of 0.86 μm.

2.1.4 Sky view factor

Many studies have proven that city geometry has a microclimate effect on the environment. Notably, they have determined that buildings affect sky shine and result in the city being unable to cool at night, thereby resulting in a UHI effect (Oke, 1981). Sky view factor (SVF) is categorized into three types: ground SVF (GSVF), roof SVF (RSVF), and total SVF (TSVF). Different locations, shapes, and sizes of buildings result in different SVFs. The SVF is defined as follows (Wenjing, Yanuar, & Perry, 2004):

$$TSVF = \sum_{\text{i=1→Ng}} GSVF_i + \sum_{\text{i=1→Nr}} RSVF_i,$$

2.1.5 Average area solar radiation

The total solar radiation (TSR) and average area solar radiation (AASR) are defined as follows:

$$\text{TSR} = \sum_{q=1}^{P} SR_q$$

$$\text{AASR} = \frac{TSR}{P} \times A,$$

where *SR* position is the view solar radiation, *p* is the number of observation points in a given cell grid, and A is the area of the cell grid.

2.1.6 LST

$$\text{T} = K\_2/ln\left(\frac{K_2}{L_\lambda} + 1\right)$$

$$L_\lambda = G_{rescale} \times DN + B_{rescale},$$

where *T* denotes the LST and L_λ is the spectral radiance at the sensor's aperture; K2 = 1260.56 K, K1 = 607.76 (W·m^2·sr·μm), Sr = steradian (SI unit of solid angle), $G_{rescale}$ = 0.055158 W·m^2·sr·μm/DN, and $B_{rescale}$ = 1.2378 (W·m^2·sr·μm).

$$T_\varepsilon = T / \left\{1 + \left[\frac{\lambda \times T}{\rho} \times \ln(\varepsilon)\right]\right\},$$

where λ is the wavelength of emitted radiance (11.5μm), ρ is 1.438 × 10^{-2} m K, and ε is the emissivity.

2.2 RESEARCH METHODS

2.2.1 OLS

The OLS model was generated, and we assumed that the spatial autocorrelation problem is not considered. The formula is expressed as follows:

$Y = X\beta + \varepsilon$, ε is error.

We used Moran's I test to validate the spatial autocorrelation in OLS and determined whether the data in space are distributed randomly or are correlated.

$$Y=X\beta +W\varepsilon+u.$$

2.2.2 SEM

The SEM is suitable for the existence of spatial autocorrelation. It produced errors in the original model. The formula is expressed as follows:

$$Y = X\beta + W\varepsilon + u,$$

where *W* denotes the spatial weights matrix and ε is the error

2.2.3 SLM

The SLM is derived from spatial proximity and is so called owing to the analogy with the time lag in time series models. The formula is expressed as follows:

$$y = \rho W y + X\beta + \varepsilon,$$

where *W* denotes the spatial weights matrix and ε is the error

2.2.4 Moran's I

Moran's I test coefficient values lie between 1 and −1. Values from 1 to 0 represent a positive correlation, indicating a cluster distribution; values from 0 to −1 represent a negative correlation, indicating dispersion. The average value indicates spatial distribution. Values close to 0 indicate a random state or irregularity in the spatial distribution (Chen, 2013).

$$Ie = \frac{-1}{n-1},$$

where *n* is number of samples and *Ie* is the expected value.

2.2.5 Test of goodness of fit

The R^2 between SLM and SEM cannot be compared because both models exhibit spatial correlation. Therefore, we used log likelihood (LIK) and the Akaike information criterion (AIC) to test goodness of fit. Higher LIK and lower

AIC values represented more effective models (Ai, 2005; Lee & Chen, 2010).

2.3 SUMMARY

Data from the aforementioned research materials were obtained using ArcGIS and GeoDa spatial statistics software, and the spatial regression coefficients were obtained using GeoDa. Table 1 provides information for each factor.

Table 1 Independent and depend variables in the regression models.

Y	LST Land surface temperature
X1	Building
X2	Average area solar radiation (AASR)
X3	Sky view factor (SVF)
X4	Normalized difference vegetation index；NDVI
X5	Water*

*Water and NDVI collinearity are too high to be considered, so we remove this factor in the regression models.

3 RESULTS

3.1 Study area and confirmation

Taichung City is the second-largest city in Taiwan and is a traffic hub. The urban areas of Taichung City have dramatically expanded over the past two decades. In recent years, Taichung City Government has proposed numerous green land planning measures. Therefore, exploring Taichung City's high-density-area LST and UHI effect has become crucial. The installation of new parks between 2015 and 2017 is expected to reduce the LST.(Figure 1)

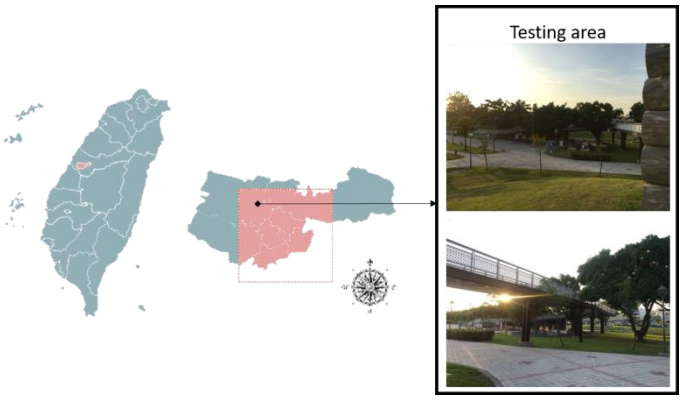

Figure1. Study area and testing area in Central Taiwan.

3.2 Results

We used three spatial regression models to explore the relationship between LST and environmental factors. Because OLS does not consider spatial lag and spatial error, space autocorrelation and other problems are evident

(Table2). The R^2 was stabilized after 2010. Additionally Moran's I indicated spatial autocorrelation in 2010 and 2015; however, the regression error was gradually distributed by the clustering state.

Table 2 The R^2 and Moran's I with different grid size.

Year	Grid size	R^2	Moran's I
2010	60m × 60m	0.495	0.5376
	120m × 120m	0.618	0.4616
	240m × 240m	0.669	0.3543
	480m × 480m	0.682	0.3457
2015	60m × 60m	0.348	0.6337
	120m × 120m	0.473	0.5266
	240m × 120m	0.398	0.3662
	480m × 480m	0.587	0.2699

Comparing SEM and SLM requires applying the test of goodness of fit. When LIK and AIC are used in the goodness-of-fit test, the model with the highest LIK and lowest AIC is the most effective. SEM and SLM involve the same method, for example, comparing SEM and SLM to determine whether the 60 m × 60 m and 120 m × 120 m grids were more favorable in 2015. The 240 m × 120 and 480 m × 480 m grids were more favorable in 2010, but their LIK and AIC values were closer in 2015, which facilitates the prediction of the 2017 values (Table3).

Table 3 LIK and AIC index with different models and data in different years.

Model	Year	Index	Grid size			
			60m×60m	120m×120m	240m×240m	480m×480m
SEM	2010	LIK	-22647	-6037	-1454	-286
		AIC	45304	12083	2917	581
	2015	LIK	-14687	-4697	-1615	-303
		AIC	29384	9404	3240	616
SLM	2010	LIK	-23326	-6364	-1549	-313
		AIC	46665	12741	3110	638
	2015	LIK	-18116	-5442	-1616	-309
		AIC	36245	10896	32445	629

This study explored the effects of environmental factors on the LSTs of four grids. We selected the SEM to predict the LST in January 2017. Green cover and LST exhibited a negative correlation, as shown in Tables 3 and 4.When the temperature gradually increases, the green cover gradually decreases. The building and the LST exhibited a positive correlation. Additionally, in recent years, buildings have used geometric designs and glass curtains. The SEM is the more effective model in 2015, as shown in Tables 4 and 5. Therefore, we assessed the accuracy of January 2017 LST predictions. Additionally, we used the models generated using the data in 2010 to predict the LST in January 2017 and compared the accuracy of the different results.

Table 4 The results of SEM with the data in 2010.

Variable	Grid size							
	60m×60m		120m×120m		240m×240m		480m×480m	
Variable	Coefficient	z-value	Coefficient	z-value	Coefficient	z-value	Coefficient	z-value
CONSTANT	21.6348	256.3170	19.3860	131.6880	16.7706	58.8055	14.2743	24.5593
BGFA	3.414×10^{-5}	5.0875	4.150×10^{-5}	8.8806	2.491×10^{-5}	8.2269	1.445×10^{-5}	7.9883
ASR	0.0028	23.4798	0.0087	22.4499	0.0205	15.3693	0.0164	4.9359
SVF	0.3646	3.4455	0.7117	3.0511	-1.0671	-1.7218	2.9835	2.0561
NDVI	-7.7319	-118.6620	-10.0017	-80.9356	-11.1460	-44.6665	-11.2905	-24.7014
LAMBDA	0.8669	221.6610	0.8287	92.8848	0.7028	29.2408	0.6937	15.0945
R	0.8011		0.8011		0.7782		0.7836	
LIK	-22646.8664		-6036.6281		-1453.5859		-285.6163	
AIC	45303.7000		12083.3000		2917.1700		581.2330	
SC	45343.8000		12117.1000		2944.5200		602.0280	

Table 5 The results of SEM with the data in 2015.

Variable	Grid size							
	60m×60m		120m×120m		24m×240m		480m×480m	
	Coefficient	z-value	Coefficient	z-value	Coefficient	z-value	Coefficient	z-value
CONSTANT	29.8865	393.0030	27.4097	206.0250	24.3735	75.7121	21.9097	39.0497
BGFA	8.501x10-5	15.8370	7.575x10-5	18.3435	5.772x10-5	17.0750	1.168x10-5	6.0073
ASR	0.0017	21.8727	0.0058	19.6406	0.0126	9.3776	0.0199	6.4745
SVF	0.2820	3.6787	1.8586	9.5284	1.0640	1.5553	2.7768	1.9497
NDVI	-4.4339	-43.2488	-7.8439	-35.3078	-1.2578	-2.5447	-13.1110	-12.4996
LAMBDA	0.9402	409.9600	0.8999	140.0440	0.7858	39.3633	0.6272	11.9228
R	0.8584		0.8097		0.6438		0.686	
LIK	-14686.8656		-4696.9315		-1615.0600		-302.8941	
AIC	29383.7000		9403.8600		3240.1200		615.7880	
SC	29423.4000		9437.3300		3267.2100		636.3790	

We used the SEM models from the data in 2010 and 2015 to predict the LST in all study areas in 2017. With the data in 2010, the results show a maximum error of approximately −6.7°C and a minimum error of approximately −5.8°C; while with the data in 2015, the results show a maximum error of approximately 3.1°and a minimum error of approximately 1.3°C (Table 6).

Table 6 The validation results of SEM models with the data in 2010 and 2015 for all study area in 2017.

Year	LST and Prediction Error	Grid size			
		60m×60m	120m×120m	240m×240m	480m×480m
SEM model from the data in 2010	Real average LST	26.997	27.007	27.032	27.045
	Prediction LST	21.201	20.657	20.466	20.319
	Error	-5.797	-6.350	-6.566	-6.726
SEM model from the data in 2015	Real average LST	26.997	27.007	27.032	27.045
	Prediction LST	29.809	29.284	30.145	28.358
	Error	2.811	2.277	3.114	1.313

We also chose a local green park, Veteran Trees Park, in the study area as the testing area to check if the errors were similar as the global area. With the data in 2010, the results show a maximum error of approximately −6.8°C and a minimum error of approximately −6.3°C; while with the data in 2015, the results show a maximum error of approximately 2.6°and a minimum error of approximately 1.7°C (Table 6).

Table 7 The validation results of SEM models with the data in 2010 and 2015 for the testing area in 2017.

Year	LST and Prediction Error	Grid size			
		60m×60m	120m×120m	240m×240m	480m×480m
SEM model from the data in 2010	Real average LST	28.215	28.130	28.048	27.835
	Prediction LST	21.706	21.353	21.356	21.539
	Error	-6.509	-6.777	-6.692	-6.297
SEM model from the data in 2015	Real average LST	28.215	28.130	28.048	27.835
	Prediction LST	30.122	29.872	30.625	29.600
	Error	1.907	1.742	2.577	1.764

4. DISCUSSION AND CONCLUSIONS

Form the aforementioned results obtained from 2015 data, the forecast 2017 average LST error is small. We additionally used the 2010 predicted average LST error for comparison.

The lower predicted accuracy of the SEM model generated from the 2010 data may be because more unintended environmental factors affect the LST, thereby making the prediction results less accurate. However, regardless of whether the smaller 60 m × 60 m grid or the larger 480 m × 480 m grid is investigated using the regression model established using data from different years, the predict model and building regression model used the sooner data then the simulation error will be the largest. Therefore, the results suggest that simulating different future urban planning programs for studying the LST impact is feasible. However, the longer the data is used in the simulation model, the less accurate the simulation results are. Future studies should simulate the future impact of the completion of the large-scale redevelopment areas in Taichung City, such as the Taichung Gateway, on the LST of its adjacent areas for UHI reduction. Urban planners can determine whether the land use planned in each district is suitable.

5. REFERENCE

Ai, C.-L. (2005). The Impacts of Geographic Factor on Residential Land Price. *Department of Economics, Shih Hsin University*.

Anselin, L. (2013). *Spatial econometrics: methods and models* (Vol. 4): Springer Science & Business Media.

Bottyn, Z., & Unger, J. (2003). A multiple linear statistical model for estimating the mean maximum urban heat island. *Theoretical and Applied Climatology, 75*(3-4), 233-243. doi:10.1007/s00704-003-0735-7

Carlson, T. N., & Ripley, D. A. (1997). On the relation between NDVI, fractional vegetation cover, and leaf area index. *Remote Sensing of Environment, 62*(3), 241-252.

Chang, Y.-l. (2010). The Impact Study of Urban Heat Island Effect Caused by Land Cover Transition. *Feng-Chia University Department of Land Management*.

Chen, K.-T. (2013). GIS Spatial Regression Analysis of Land Price Variation -An Example of Eastern Tainan City. *Department of Earth Sciences, NCKU*, 1-119.

Chun, B., & Guldmann, J. M. (2014). Spatial statistical analysis and simulation of the urban heat island in high-density central cities. *Landscape and Urban Planning, 125*, 76-88. doi:10.1016/j.landurbplan.2014.01.016

Landsberg, H. E. (1981). *The urban climate* (Vol. 28): Academic press.

Lee, R.-Y., & Chen, S.-I. (2010). The Spatial Analysis of the Robbery Hot Spot and Crime Location in Taichung City. *Journal of Geographical Research, (53), 2010*(53), 23-48.

Lin, C.-M. (2010). The Influence and Environmental Meaning of Urban Heat Island Effect *Journal of Ecology and Environmental Sciences, 3*(1), 1-15.

Lin, H.-T., Kuo, H.-C., Lee, K.-p., Chen, T.-C., & Chen, K.-T. (2001). Experimental Analyses on Urban Heat Island Effect and Its Improvement Strategies in Coastal Cities of Taiwan--Analyses for Tainan, Kaoshoung and Hsinchu. *City and Planning(2001)； Vol28, NO3， P323 - 341*.

Lu, Y.-L. (2008). Applying LST of Remote Sensing to Explore the Relationship Between Unban Heat Island Effects and Spatial Development of SocialEconomic. *Department of Urban Planning*, 1-62.

Oke, T. R. (1981). Canyon geometry and the nocturnal urban heat island: comparison of scale model and field observations. *International Journal of Climatology, 1*(3), 237-254.

Song, J., Du, S., Feng, X., & Guo, L. (2014). The relationships between landscape compositions and land surface temperature: Quantifying their resolution sensitivity with spatial regression models. *Landscape and Urban Planning, 123*, 145-157.

Wenjing, L., Yanuar, S., & Perry, P. (2004). GIS analysis for the climatic evaluation of 3d urban geometry: The development of GIS analytical tools for sky view factor: GISDECO.

Xu, H. (2006). Modification of normalised difference water index (NDWI) to enhance open water features in remotely sensed imagery. *International journal of remote sensing, 27*(14), 3025-3033.

6. ACKNOWLEDGEMENTS

We appreciate the Ministry of Science and Technology, Taiwan, for financial support of this research under contract 106-2627-M-035 -002 -.